



# Self-Leveling Laser for Direction Marking System

Nur Hazliza Ariffin<sup>1</sup>, Norhana Arsad<sup>1,2\*</sup>, Azri Hariz Ahmad<sup>1</sup>, Badariah Bais<sup>1,2</sup>, Noorfazila Kamal<sup>1,3</sup>, Norazreen Ab Aziz<sup>1,2</sup>, Siti Salasiah Mokri<sup>1,3</sup> and Raihanah Mohd Mydin<sup>4</sup>

<sup>1</sup>Program of Electric & Electronic Engineering,

<sup>2</sup>Centre of Advanced Electronic & Communication Engineering,

<sup>3</sup>Pusat Kejuruteraan Sistem Bersepadu dan Teknologi Termaju,

Faculty of Engineering and Built Environment,

<sup>4</sup>Faculty of Social Sciences & Humanities,

Universiti Kebangsaan Malaysia, 43600 Bangi, Selangor, Malaysia

\*Corresponding author E-mail: [noa@ukm.edu.my](mailto:noa@ukm.edu.my)

## Abstract

The laser has the ability to radiate a fine shaft of light within a certain distance, yet it will produce excess infrared light that is invisible to the eye. Direct exposure towards the infrared light is extremely dangerous as it can cause serious eye damage. Therefore a self-leveling laser for direction marking system is proposed to control the movement of the laser and to reduce the risk of direct exposure to the eye. The development of the system is achieved with a Micro-Electro-Mechanical System (MEMS) gyroscope and accelerometer to support the structure orientation of the mounted laser on a servo motor before the laser emits light. Data from both sensors are successfully merged through a complementary filter with a filter factor,  $\alpha = 0.97$ . Moreover, the light intensity of 532 nm green and 650 nm red wavelength laser diodes were measured using a spectrometer and the comparison shows that the green laser has a narrower linewidth as the distance is increased.

**Keywords:** Gyrometer; Laser, MEMS, Servo motor, Spectrometer.

## 1. Introduction

The laser is a designated tool which amplifies the intensity of light in order to produce a laser beam with specific frequency and wavelength<sup>1</sup>. As laser technology expands, the laser devices become cheaper<sup>2</sup> and these lead to the increased usage of laser devices in a variety of sectors<sup>3,4</sup> such as commercial laboratories<sup>5</sup>, military<sup>6-10</sup>, and in medical areas including construction. In addition, the laser has the ability to create a visible direction line and is considered a great tool to mark the direction. However, there are a rising number of people losing vision from the exposure to laser pointers<sup>11-15</sup>. These are due to the harmful utilization of the laser devices that bring complications and may cause humans to suffer serious retinal damage from direct exposures to unseen light<sup>16-20</sup>.

The objective of this work is to build a prototype for marking the direction using the laser to limit the laser exposure in order to reduce the risk of severe injury. Hence, an implementation of safety measures to appropriately steer the laser source forming the directional line pointing towards the target direction is required for quality assurance. Therefore, a motorized laser for direction marking system is achieved with a self-leveling Micro-Electro-Mechanical System (MEMS) gyroscope and accelerometer. The selected MEMS in this work is the MPU6050 which comprises a combination of a three-axis gyroscope and accelerometer.

MEMS technology evolves when the gyroscope and accelerometer become commercially accessible, making angle measurement cheaper due to its low power consumption<sup>21-24</sup>. The MEMS gyroscope is used to measure the angular rate of rotation<sup>25, 26</sup> through the rate of change in orientation angle over time (angular velocity) with a measurement unit of degree per second. The angular rate signal must be integrated with respect to time to obtain a readable angle<sup>27,28</sup> but the accuracy will degrade rapidly with time where the measured angle did not return to zero when the MEMS gyroscope is in a static condition. Due to that reason, the error needs to be handled appropriately in order to obtain an accurate angle estimation. Combining the MEMS gyroscope and accelerometer via Kalman filter<sup>29</sup> to improve accuracy is a common practice and is widely used in robotics application. However, these filters are computationally expensive. They are too complex with long computational time, making it hard to program on a certain 8-bit microcontroller that makes them difficult to run in current low-expense mobile devices.

A complementary filter which consists of high pass and low pass filters is an alternative way with a less complex technique to merge sensor readings<sup>30, 31</sup>. The main concept of the complementary filter is the robustness of one sensor will be used to curb the weaknesses of the other sensor. Therefore, building on the above, a digital complementary filter is developed to cater the issues where it combines the best attributes of the MPU6050, MEMS gyroscope, and the accelerometer.

The remainder of the paper is organized as follows: Section 2 presents system hardware design and software supported by the integrated development environment (IDE). Section 3 shows the setup assembly using a spectrometer for light intensity measurement. The measurement results are presented in Section 4. Section 5 summarizes the results of this work and draws conclusions.

## 2. System Hardware Design

The MPU6050 MEMS gyroscope and accelerometer depicted in Figure 1 is used to demonstrate the auto-leveling of the direction marking system. 3.3 volts of power supply from the Arduino Mega microcontroller is applied to activate the MPU6050 and it communicates with it through the I2C protocol.

The microcontroller Arduino Mega serves as a processing module and controls the rotation of the joined two servo motors at the MPU6050 tilt and pan unit for stability. The MPU6050 will sense the degree of inclination via the sensor when an application was tilted. The microcontroller will receive the signal from the sensor and sends a signal to the servo motor to move back to a stable position to ensure the laser is in the 90° position. The connection setup between the MPU6050 and Arduino Mega is as Table 1 while Figure 2 shows the block diagram of the direction marking system.



Fig.1: MPU6050 MEMS gyroscope and accelerometer

Table 1: The connection setup between MPU6050 and Arduino Mega

| MPU6050 | Arduino Mega        |
|---------|---------------------|
| VCC     | 5 V                 |
| GND     | GND                 |
| SCL     | Pin 21 (SCL)        |
| SDA     | Pin 20 (SDA)        |
| INT     | Pin 2 (Interrupt 0) |



Fig.2: Block diagram of the direction marking system

In the data sheet of the MPU6050 gyroscope, it is stated that when the gyroscope is rotating at one degree per second (dps), the output will be 65.5. So, if the gyroscope is rotating around the yaw axis at six degrees per second (6°/s), the output of the gyroscope is 393. The calculation is computed as follows.

EQUATION 1. For the angular velocity=6°/s, the roll, pitch, and yaw axis output,  $G_{out}=6^{\circ}/s \times 65.5$  is 393 of gyroscope raw data. For convenience, the raw data will be divided by 65.5 which determines the measured output in dps. A static test is performed to investigate the performance of the MPU6050 gyroscope and it is found that the measured output implies that the sensor is moving. Therefore, the MPU6050 gyroscope needs to be calibrated and the algorithm in the IDE is presented below.

```
// Calibration MPU6050 gyroscope
1  int average;
2  for (average=0;average<2000;average++)
3  {
4    read_mpu_6050_data();
5    Gout_x_cal += Gout_x;
6    Gout_y_cal += Gout_y;
7    Gout_z_cal += Gout_z;
8    delay(3);
9  }
10  Gout_x_cal /= 2000;
11  Gout_y_cal /= 2000;
12  Gout_z_cal /= 2000;
```

The flow of the algorithm is as follows: 2000 readings of the gyroscope will be collected and the mean value is stored for the offset. Then, the mean value subtracts this from the raw output.

### 3. System Software Design

The MPU6050 gyroscope measures angular motion in the measurement unit of degrees per second. The digital complementary filter is implemented in such a way that the strength of one sensor will be used to overcome the weaknesses of the other sensor, as the sensors are complementary to each other. The block diagram in Figure 3 illustrates two inputs; the accelerometer angle estimation and the gyroscope angular rate. A low pass filter will filter the high-frequency signals when the accelerometer senses the condition of vibration. The input of the gyroscope angular rate will be integrated to yield an attitude angle before it feeds into the high pass filter to negate the effect of drift. Both the high-pass and low-pass filters work simultaneously, then both signals are summed together. The programming code is as presented and shown previously in<sup>24</sup>.

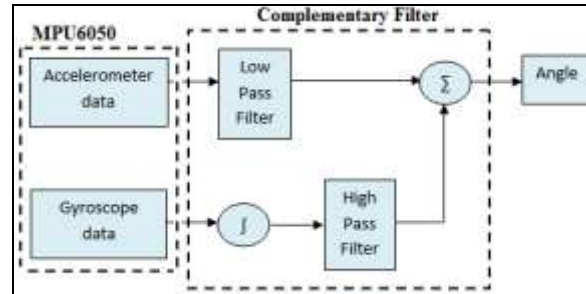


Fig.3: Block diagram of the digital complementary filter

### 4. Setup of Light Intensity Test

The measurement of the light intensity level of the laser is carried out according to the output power and color of the laser diode. There are two different lasers with the wavelengths of 532 nm for the green diode laser and 650 nm for the red diode laser. The specification of both lasers is presented as per below Table 2.

Table 2: Specification of Tested Laser

| Type of laser | Wavelength | Output Power |
|---------------|------------|--------------|
| Green         | 532 nm     | 30 mW        |
| Red           | 650 nm     | 5 mW         |

The intensity of laser light was measured using a device called a spectrometer. The spectrometer is used to measure the intensity of light according to a specific wavelength. The wavelengths that can be detected by the spectrometer are in the range from 190 nm up to 1100 nm. Normally it is operated in the region of the electromagnetic spectrum that has been identified.

In this testing, the intensity of laser light was determined by the change in the specified distance of the laser. The distances used are 0.8 m, 1.0 m, 1.2 m, 1.4 m, 1.6 m, 1.8 m and 2.0 m. The power source to both lasers is supplied from the constant current driver circuit at the same voltage of 9 V. The test was conducted in a dark room to avoid interference from other light sources to ensure a correct measurement reading because the spectrometer is very sensitive to light. Laser emissions are capable of causing severe eye damage if viewed directly, hence, safety eyewear is compulsory during the experiment as safety measure. The performed test is defined as follows.

STEP 1. A track was measured and labeled at a specific distance in the unit of meter to ensure that the laser beam points straight to the spectrometer as captured in Figure 4.

STEP 2. Then, the laser was placed on a holder and the laser must be in parallel condition with the attenuator to ensure that it receives the laser light. This needs to be done correctly so that the light intensity can be measured by the spectrometer. Figure 5 showed the green diode lasers that were placed in the holder and emitted beams parallel to the attenuator.

STEP 3. The measured data via the spectrometer will be transferred to a software called SpectraSuite. This software will tabulate the data and give a graphical intensity of light versus wavelength.

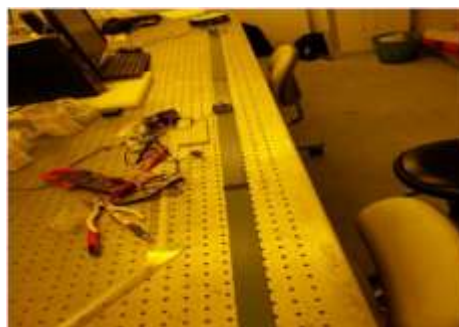


Fig.4: Light intensity measurement setup

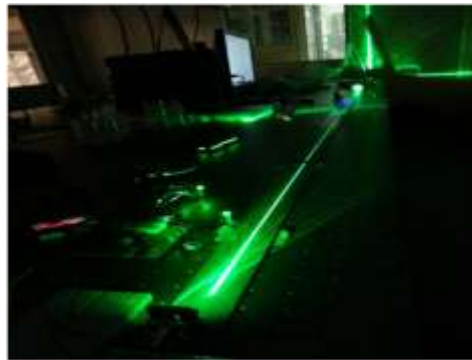


Fig.5: Measurement process of green laser in a dark room

### 5. Results and Discussion

The signal conditioning measured from the MEMS gyroscope and accelerometer is connected to the input device of Arduino Mega via the I2C communication medium. The measurement graph is captured by importing data from Arduino to Excel (in real-time) via the Parallax Data Acquisition tool (PLX-DAQ) software. The results of the raw data accelerometer and gyroscope in real-time captured via the PLX-DAQ are presented in<sup>24</sup>.

The presented graph of Figure 10 in reference<sup>24</sup> reveals a clear trend of accelerometer sensibility to noise while the gyroscope experienced some drift angles, where in reality it is in a static condition with zero angles. This clearly proves that both gyroscope and accelerometer requires a filter to ensure the output is free of interference. A factor value will be tuned in order to find the best value where a simple rotation along the X-axis is done throughout the whole experiment.

The obtained values from the preliminary analysis are shown in Figures 11, 12, 13 and 14 of reference<sup>24</sup> for different constant settings of the complementary filter, and the best factor value of 0.97 is chosen. Hence, the system is proven to be in a stable position when the servo is in 90° position as presented in Table 3. The light intensity test between the red and green diode lasers shows that both are at the same level of 16000 numbers despite different distances. However, the differences can only be identified by viewing the wide gaps of the laser light intensity graph. The width of the line represents the dilation of the diode laser pulse, when the diode laser pulse gap width is increased, the light intensity rate will be decreased.

Table 3: Experimental Results of Servo Motor

| X-axis in degree | Y-axis in degree | Servo motor in X-axis | Servo motor in Y-axis |
|------------------|------------------|-----------------------|-----------------------|
| 0                | 0                | 90                    | 90                    |
| 2                | 0                | 82                    | 90                    |
| 4                | 0                | 74                    | 90                    |
| -2               | 0                | 98                    | 90                    |
| -4               | 0                | 106                   | 90                    |
| 0                | 2                | 90                    | 98                    |
| 0                | 4                | 90                    | 106                   |
| 0                | -2               | 90                    | 82                    |
| 0                | -4               | 90                    | 74                    |

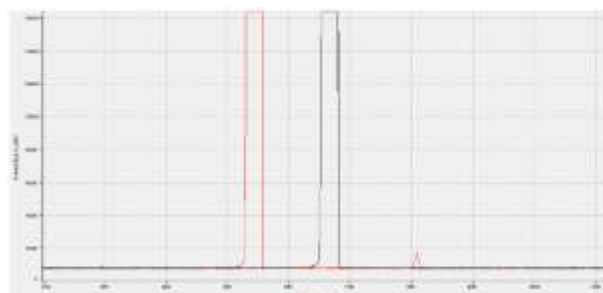


Fig.6: The intensity graph of green and red diode lasers at 1.0 m distance

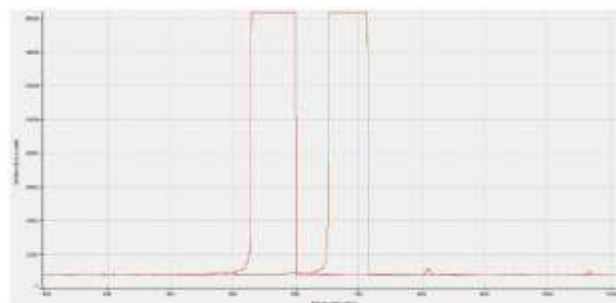


Fig.7: The intensity graph of green and red diode lasers at 1.8 m distance

**Table 4:** Linewidth of green and red diode laser

| Distance, m | Linewidth for red diode laser, nm | Linewidth for green diode laser, nm |
|-------------|-----------------------------------|-------------------------------------|
| 0.8         | 9.45                              | 10.64                               |
| 1.0         | 25.53                             | 26.20                               |
| 1.2         | 80.41                             | 32.41                               |
| 1.4         | 89.03                             | 56.70                               |
| 1.6         | 98.63                             | 78.08                               |
| 1.8         | 59.88                             | 70.36                               |
| 2.0         | 75.85                             | 83.74                               |

Figures 6 and 7 represent the graphs of the green and red diode lasers with different distances using the spectrometer. The red graph lines show the green diode laser while the yellow graph lines are the graphs of the red diode laser. The graphs are analyzed by calculating the width of each line of the graph. The result shows that the width of the green diode laser line is smaller than the laser light as the distance increases. Table 4 shows the complete data and revealed that when the distance is further away, the width of the line will be wider, indicating that widening has occurred.

From Table 4, the linewidth of the red diode laser is broader compared to the green diode laser, meaning that the red diode laser beam is more scattered when the distance increases. Hence, the green diode laser is chosen in the developed prototype for the direction marking system and the overall stability of the self-leveling system using a MEMS gyroscope and accelerometer is satisfied.

## 6. Conclusions

The presented work demonstrates a self-leveling system with the utilization of a MEMS gyroscope and accelerometer for a direction marking system. Based on the standard testing of light intensity using a spectrometer, it is observed that the green diode laser has a higher intensity and thus chosen for the self-leveling application. Moreover, experimental results also proved that drift can be filtered at a factor value of 0.97 without any difficulty by using a complementary filter via the Arduino Software (IDE) for system stability.

## Acknowledgement

This work is financially supported by the Centre for Collaborative Innovation (PIK), Universiti Kebangsaan Malaysia (UKM) through the grant INOVASI-2017-10, AP-2015-015 and FRGS/1/2016/TK04/UKM/02/7.

## References

- [1] William T. Silvast. Laser. Light of a Million Uses University of Central Florida Orlando, Florida. Fundamental of Photonics. (2003).
- [2] Ying WU, Ping-Bo Ouyang and Luosheng Tang. Journal of Clinical & Experimental Ophthalmology, 5(1)(2014) 1-3.
- [3] Radha Shenoy, Alexander A Bialasiewicz, Asoka Bandara, and Roshini Isaac. Retinal damage from laser pointer misuse – case series from the military sector in Oman. Middle East African Journal Ophthalmol, 22(3)(2015) 399-403
- [4] Mainster MA, Stuck BE and Brown J. Assessment of alleged retinal laser injuries. Journal American Medical Association Arch Ophthalmol. (122)(2004) 1210-1217.
- [5] Allen RD, Brown J, Jr, Zwick H, Schuschereba ST, Lund DJ and Stuck BE. Laser-induced macular holes demonstrate impaired choroidal perfusion. Journal Retina. (24)(2004) 92-97.
- [6] ANSI Z136.1-2000. Washington, DC: American National Standards Institute. American National Standard for the Safe Use of Lasers. (2000)
- [7] Wyrsh S, Baenninger PB and Schmid MK. Retinal injuries from a handheld laser pointer. New England Journal of Medicine. (363)(2010) 1089-1091.
- [8] Robertson DM, McLaren JW, Salomao DRand Link TP. Retinopathy from a green laser pointer: A clinic pathologic study. Middle East African Journal Ophthalmol. (123)(2005) 629-633.
- [9] Alsulaiman SM, Alrushood AA, Almasaud J, Alzaaidi S, Alzahrani Y and Arevalo. High-power handheld blue laser-induced maculopathy: the results of the king khaled eye specialist hospital collaborative retina study group. Middle East African Journal Ophthalmol. (121)(2014) 566-572.
- [10] M. H. Lee, K. Fox, S. Goldwasser, D.W.M. Lau, B. Aliahmad and M. Sarossy. Green lasers are beyond power limits mandated by safety standards. IEEE 38th Annual International Conference of the Engineering in Medicine and Biology Society, Orlando, USA (2016).
- [11] Jeon, S. and W.K. Lee. Inner retinal damage after exposure to green diode laser during a laser show. Journal Clinical Ophthalmol. (8)(2014) 2467-2470.
- [12] N. Raof, J. O'Hagan, N. Pawlowska and F. Quhill. 'Toy' laser macular burns in children. Journal Eye (Lond), 28(2)(2014) 231-234.
- [13] Dirani. Bilateral macular injury from a green laser pointer. Journal Clinical Ophthalmol. (7)(2013) 2127-2130.
- [14] S. Ross. Laser pointers not toys, optometrists warn, after Tasmanian teenager damages eyes. (2015).
- [15] T. Ueda, I. Kurihara, and R. Koide. A case of retinal light damage by green laser pointer (Class 3b). Journal Clinical Ophthalmol. 55(4)(2011) 428-430.
- A. Alhalel, Y. Glovinsky, G. Treister, E. Bartov and M. Blumenthal. Long-term follow-up of accidental parafoveal laser burns. Journal Retina. 13(2)(1993)152–154.
- [16] Y. S. Cai, D. Xu, X. Mo. Clinical, pathological and photochemical studies of laser injury of the retina. Journal Health Phys. 56(5)(1989) 643–646.
- [17] M. Modarres-Zadeh, M. M. Parvares, S. Pourbabak, G. A. Peyman. Accidental parafoveal laser burn from a standard military ruby range finder. Journal Retina. 15(4)(1995) 356–358.
- [18] Y. Barkana, M. Belkin. Laser eye injuries. Survey of Ophthalmology. 44(6)(2000) 459-478.
- [19] T. Nakamura, T. Nishizawa, M. Hagiya, T. Seki and M. Shimonishi. Molecular cloning and expression of human hepatocyte growth factor. Journal Nature. 342(6248)(1989) 440-443.
- [20] A.R. Schofield, A.A Trusov and A.M Shkel. Versatile vacuum packaging for experimental study of resonant MEMS. IEEE 23rd International Conference on Micro Electro Mechanical Systems (MEMS), Wanchai, Hong Kong, (2010) 516-519.
- [21] T.S. Woon, T. Kang and J.G. Lee. Controller Design of a MEMS Gyro-Accelerometer with a Single Proof Mass. International Journal of Control, Automation, and Systems, (6)(2008) 873-883.
- [22] Yu Liu, Song Liu, Changwen Wang and Le Wang. A new northseeking method based on MEMS gyroscope. International Frequency Sensor Association Journal Sensors and Transducers, (178)(2014) 14-19.
- [23] Ariffin NH, Arsad N, Jumat F, Zain MFM, MSD & Bais B (2018), Vector algebra qibla detection in an indoor, semi-open and outdoor environment. Journal of Engineering Science and Technology, 13, 1573-1586.

- [24] Park S, Horowitz and Tan CW. Dynamics and control of a MEMS angle measuring gyroscope. IEEE Conference of sensors and actuators, Yokohama, Japan, (2008) 56-63.
- [25] Chi CY and Chen TL. MEMS gyroscope control systems for direct angle measurements. IEEE Conference of Sensor, Christchurch, New Zealand, (2009) 492-496.
- [26] Painter C and Shkel A. Experimental evaluation of a control system for an absolute angle measuring micromachined gyroscope. 4th IEEE Conference on sensors, Irvine, USA, (2005) 1084-1087.
- [27] Hu YD, Sun YR, Jian L and Wu C. Combined heading technology in vehicle location and navigation system. IEEE International Conference on Software Engineering and Service Sciences, Beijing, China, (2010) 53-57
- [28] Robert, Tarek H and Jean MP. Complementary filter design on the special orthogonal group. 4th IEEE Conference on Decision and Control and The European Control, Seville, Spain, (2005) 1477 1484.
- [29] Pascoal A, Kaminer I and Oliveira P. Navigation system design using time-varying complementary filters. IEEE Transactions on Aerospace and Electronic Systems, New York, (2000)1099-1114.
- [30] Armando AN, Douglas GM, Victor CSC and Mario FC. Adaptive complementary filtering algorithm for mobile robot localization. Journal of the Brazilian Computer Society, 15(3)(2009)19-31.